Polycaprolactone nanofibers as an adjuvant strategy for Tamoxifen release and their cytotoxicity on breast cancer cells

Ana Pinzón-García [1], **Ruben Sinisterra** [1], **Maria Cortes** [2], **Fredy Mesa** [Corresp., 3], **Sandra Ramirez Clavijo** [3]

[1] Chemistry Department, Instituto de Ciências Exatas, Universidade Federal de Minas Gerais, Belo Horizonte, Brazil

[2] Restorative Dentistry Department, Faculty of Dentistry, Universidade Federal de Minas Gerais, Belo Horizonte, Brazil

[3] Faculty of Natural Sciences, Department of Biology, Universidad del Rosario, Bogotá, Colombia

Corresponding Author: Fredy Mesa
Email address: fredy.mesa@urosario.edu.co

Breast cancer is the second leading cause of death in women, and tamoxifen citrate (TMX) is accepted widely for the treatment of hormone receptor–positive breast cancers. Several local drug-delivery systems, including nanofibers, have been developed for antitumor treatment. Nanofibers are biomaterials that mimic the natural extracellular matrix, and they have been used as controlled release devices because they enable highly efficient drug loading. The purpose of the present study was to develop polycaprolactone (PCL) nanofibers incorporating TMX for use in the treatment of breast tumors. Pristine PCL and PCL-TMX nanofibers were produced by electrospinning and characterized physiochemically using different techniques. In addition, an in vitro study of TMX release from the nanofibers was performed. The PCL-TMX nanofibers showed sustained TMX release up to 14 h, releasing 100% of the TMX. The Resazurin reduction assay was used to evaluate the TMX cytotoxicity on MCF-7 breast cancer cell line and PBMCs human. The PCL-TMX nanofiber was slightly cytotoxic in PBMCs and highly toxic in the MCF-7. Based on these results, the PCL-TMX nanofibers developed have potential as an alternative for chronic TMX use for breast cancer treatment without affecting other cells or tissues.

Polycaprolactone nanofibers as an adjuvant strategy for Tamoxifen release and their cytotoxicity on breast cancer cells

A. D. Pinzón-García[1], R. D. Sinisterra[1], M. E. Cortés[2], F. Mesa[3, £], S. Ramírez-Clavijo[3,*]

[1] Chemistry Department, Instituto de Ciências Exatas, Universidade Federal de Minas Gerais, Av. Presidente Antônio Carlos 6627, Belo Horizonte, MG, CEP 31270901, Brazil
[2] Restorative Dentistry Department, Faculty of Dentistry, Universidade Federal de Minas Gerais, Av. Presidente Antônio Carlos 6627, Belo Horizonte, MG, CEP 31270901, Brazil
[3] Universidad del Rosario, Faculty of Natural Sciences, Department of Biology, Carrera 24 # 63C-69, Bogotá D.C., 111221, Colombia

Corresponding Author:
F. Mesa[£]
S. Ramirez-Clavijo*
Email address: fredy.mesa@urosario.edu.co; sandra.ramirez@urosario.edu.co

Abstract

Breast cancer is the second leading cause of death in women, and tamoxifen citrate (TMX) is accepted widely for the treatment of hormone receptor–positive breast cancers. Several local drug-delivery systems, including nanofibers, have been developed for antitumor treatment. Nanofibers are biomaterials that mimic the natural extracellular matrix, and they have been used as controlled release devices because they enable highly efficient drug loading. The purpose of the present study was to develop polycaprolactone (PCL) nanofibers incorporating TMX for use in the treatment of breast tumors. Pristine PCL and PCL-TMX nanofibers were produced by electrospinning and characterized physiochemically using different techniques. In addition, an in vitro study of TMX release from the nanofibers was performed. The PCL-TMX nanofibers showed sustained TMX release up to 14 h, releasing 100% of the TMX. The Resazurin reduction assay was used to evaluate the TMX cytotoxicity on MCF-7 breast cancer cell line and PBMCs human. The PCL-TMX nanofiber was slightly cytotoxic in PBMCs and highly toxic in the MCF-7. Based on these results, the PCL-TMX nanofibers developed have potential as an alternative for chronic TMX use for breast cancer treatment without affecting other cells or tissues.

Introduction

Breast cancer is the second leading cause of death in women, after lung cancer ("International Agency for Research on Cancer," 2018). Treatment strategies for this disease include surgery, radiation therapy, chemotherapy, hormonal therapy, and targeted therapy, often applied in

combination. Endocrine therapy is the treatment of choice for patients with hormone receptor–positive (HR+) breast cancer.

Breast cancer subtypes are defined by the expression of estrogen (ER) and progesterone (PR) receptors and the status of the HER-2 gene, which may be amplified. Breast cancer cell lines with molecular profiles similar to those of tumors are used to evaluate the effects of anticancer drugs in vitro. The MCF-7 cell line derives from the pleural effusion of a patient with breast adenocarcinoma and represents the luminal A breast cancer subtype because it has the same molecular profile (ER+, PR+, normal HER-2 status). The use of anti-ER drugs, such as tamoxifen (TMX), for the treatment of HR+ (ER+ and PR+) breast cancers is widely accepted (Johnston et al., 2016).

TMX, also known as 4-hydroxytamoxifen, is a nonsteroidal compound that selectively modulates the ER with antagonistic or agonist action, depending on the organ on which it acts (Salami & Karami-Tehrani, 2003). It is an agonist in the liver, uterus, and bones, and an antagonist in the brain and mammary glands and vasomotor symptoms (Sestak et al., 2006). TMX has been used to stop the proliferation and inducing apoptosis of breast tumor cells through its anti-ER action (Mandlekar & Kong, 2001; Salami & Karami-Tehrani, 2003).

TMX has cytostatic and cytotoxic properties in the MCF-7 breast cancer cell line, not only stopping proliferation and inducing apoptosis, but also inducing differentiation and reducing cholesterol synthesis (Kedjouar et al., 2004; Medina, Favre & Poirot, 2004); it also modulates immunity in patients with breast cancer (Robinson et al., 1993; Behjati & Frank, 2009). Compared with those of healthy controls, lymphocytes from women with breast cancer treated with TMX showed significantly reduced killer activity, associated with a decrease in the absolute number of CD4-type lymphocytes, and a greater proliferation response in the presence of the concanavalin A mitogen (Rotstein et al., 1988; Robinson et al., 1993; Behjati & Frank, 2009). TMX is also effective against Ebola virus (De Clercq, 2015) and human immunodeficiency virus (Laurence, Cooke & Sikder, 1990) infections, and a recent review highlighted its benefits in the treatment of respiratory diseases, such as coronavirus disease pneumonia (Salman et al., 2020). TMX and its active metabolites have prolonged serum half-lives, and higher doses have not been associated with improved outcomes; lower dosages have not been tested adequately. Furthere is established in the literature that chronic TMX use (for ≥5 years) could reduce the risk of death from PR+ ER+ breast cancer (Salami & Karami-Tehrani, 2003; Karn et al., 2010; Group (EBCTCG), 2011; Hong et al., 2016; Drăgănescu & Carmocan, 2017) but when is used with potent inhibitors of CYP2D6 could be a risk of mortality (Donneyong et al., 2016).

Furthermore, it is

It is well known that the nanometric scale devices used in current research for the prevention, treatment and diagnosis of diseases such as cancer are mostly natural or synthetic polymers. The

allowable

desirable properties for these materials are biocompatibility, biodegradability, allow controlled release of active agents and ~~present~~ similarity to the native extracellular matrix of human tissues and cells (Venugopal, Zhang & Ramakrishna, 2005; Caracciolo et al., 2011; Rogina, 2014; Mochane et al., 2019). At the same time, local delivery systems have the advantage over systemic therapy of continuous drug delivery at higher concentrations directly to target sites. The benefits of these systems include improved patient compliance, the reduction of toxic effects and systemic complications (Vyas, Sihorkar & Mishra, 2000; Jain et al., 2008; Joshi et al., 2016), mimicking of the natural extracellular matrix (ECM), and highly efficient drug loading for controlled release. Nanoscale systems, such as those in which nanofibers are employed, may present a promising opportunity for the efficient treatment of solid tumors.

Electrospun nanofibers are nanometric structures produced with synthetic or natural elements that create continuous filaments with a maximum diameter of 500 nm (Caracciolo et al., 2011). These materials are preferably biodegradable, to avoid the use of additional systems for their removal. The simplest use of nanofibers as a local drug release system involves the preparation of a polymer solution and its mixing with the drug, followed by nanofiber manufacture. Among numerous methods, electrospinning is becoming the main technique for the production of materials and carpets made of nano-polymer fibers and metal oxide (Barnes et al., 2007; Duque, Rodriguez & Lopez, 2013; Rogina, 2014; Li et al., 2019). This method is simple, versatile, common, and economical (Rogina, 2014); it is performed in an electrospinning machine, which enables the use of different compounds and control of manufacturing parameters to determine the diameter, size, and porosity of the continuous nanofibers produced (Barnes et al., 2007). Various biopolymers have been used for tailored biomedical applications (Mochane et al., 2019).

Most nanometric-scale devices used in current research on the prevention, diagnosis, and treatment of diseases such as cancer are made of natural or synthetic polymers. Desirable properties for these materials are biocompatibility, biodegradability, capacity for controlled release of active agents, and similarity to the native ECM of human tissues and cells (Venugopal, Zhang & Ramakrishna, 2005; Caracciolo et al., 2011; Rogina, 2014; Mochane et al., 2019). Poly (ε-caprolactone) (PCL), a semi-crystalline aliphatic polyester, is the most commonly used synthetic polymer in medical applications because it biodegrades slowly and is biocompatible, given its similarity to natural tissue components such as collagen fibers and ECM and diameters of 50–500 nm (Venugopal, Zhang & Ramakrishna, 2005; Barnes et al., 2007). PCL has good mechanical properties and thermal stability and is easy to process, compatible with hard and soft tissues, and accepted by the US Food and Drug Administration as a drug-delivery vehicle (Song et al., 2018). It has been used to develop devices for anticancer molecule release, an emerging promising alternative for cancer treatment (Monteiro et al., 2017).

In the present study, we developed PCL-pristine (P) and PCL-TMX nanofibers by electrospinning (Vitchuli et al., 2011) for local drug delivery to solid breast tumors. The nanofibers were

characterized by scanning electron microscopy (SEM), Fourier-transform infrared spectroscopy (FTIR) and attenuated total reflectance infrared spectroscopy (FTIR-ATR), X-ray powder diffraction (XRD), thermal analysis, and contact angle measurement. Resazurin assays (Escobar, 2010) were used to assess their cytotoxic effects on MCF-7 cells and peripheral PBMCs from a healthy donor.

Move definition from line 199 to here

Materials & Methods

Materials

PCL with molecular weights of 43,000–500,000 was purchased from Polysciences, Inc. (USA). TMX was supplied by Araujo Drug Supply S.A. (Brazil). Dichloromethane (DCM; 99.5%) and methanol (MetOH; 99.8%) were acquired from Vetec (Brazil). All reagents were of analytical grade and were used as received.

Preparation of PCL Nanofiber Solutions and Electrospinning

To prepare the PCL-P and PCL-TMX polymer solutions, 800 mg PCL was dissolved in 10 mL DCM/MetOH mixture (50%/50% v/v) in each case. For the PCL-TMX solution, 15 mg TMX was added. The solutions were agitated for 12 h at 25.0°C before use.

Each polymer solution was loaded into a 10-mL standard plastic syringe fitted with a 27-G blunted stainless-steel needle using a syringe pump (PHD 2000; Harvard Apparatus). The distance between the needle and the aluminum foil–wrapped collector was set at 15 cm, and electrospinning was performed with a solution flow rate of 10 mL/h and voltage of 20 kV generated by a high-voltage power supply (Gamma High Voltage, USA). The resulting nanofibers were collected and stored for physicochemical characterization and microbiological and cytotoxicity testing.

Physicochemical Characterization

The conditions for the physicochemical characterization of the PCL and PCL-TMX nanofibers were similar and adjusted according to (Ramírez-Agudelo et al., 2018; Dias et al., 2019).

earlier studies

Nanofiber morphology was analyzed by scanning electron microscopy (SEM) (FEG-Quanta 200; FEI) with an accelerating voltage of 20 kV. Before analysis of SEM images, each nanofiber sample was coated with a 5-nm-thick layer of gold using a sputter coater (MD20; Bal-Tec). The average nanofiber diameter was calculated from at least 100 measurements obtained with Image J software (National Institutes of Health, Bethesda, USA). ATR was performed with a spectrophotometer (Spectrum 1SR; Perkin Elmer) equipped with a universal ATR sampling accessory and a diamond top plate. The FTIR-ATR spectra of the PCL-P and PCL-TMX

nanofibers and TMX were obtained in the region of 4000–650 cm^{-1}, with four scans obtained per sample at a resolution of 4 cm^{-1}. The data were analyzed with the Spectrum software provided with the instrument (Perkin Elmer). The XRD patterns of the nanofibers were visualized using an X-ray diffractometer (XRD-7000; Shimadzu) with Cu Kα λ = 0.154051 radiations over a 2θ range of 4–60° at a scanning speed of 2θ/min. Thermogravimetric and differential thermogravimetric analysis (TGA/DTG) was performed using a TGA Q5000 device (TA Instruments, USA) with sample heating at a rate of 10°C/min from 25°C to 600°C and under an N_2 flow rate of 50 mL/min. The TG curves represent the thermal degradation of the samples. The data were processed using the software supplied with the instrument (Universal Analysis 200; TA Instruments).

A contact angle measuring system (SEO Phoenix 300 Touch) was used to determine nanofiber wettability. The nanofibers were placed on a sample stand, and water was dropped onto their surfaces while a camera recorded an image. The Surfaceware 9 software was used to determine the average contact angle.

To evaluate the drug release profile of the PCL-TMX nanofibers (loaded at 25.5 μg TMX/mg nanofiber approximately), approximately 15 mg of nanofibers was cut into specimens (15 × 15 mm), which were placed into Eppendorf tubes. The tubes were then incubated at 37°C in 2 mL phosphate-buffered saline (PBS; pH 7.4) with 0.01% Sodium Dodecyl Sulfate (SDS) for increasing the TMX solubility, in a thermostatic shaker at 50 rpm. Samples (2 mL) were removed at 0.5, 1, 2, 4, 8, 10, 24, 48, 72, 120, and 144 h for the quantification of TMX release; after each analysis, the same volume of fresh PBS solution was added to the tube. The amount of TMX released was determined using an ultraviolet–visible (UV-vis) spectrophotometer (Multiskan Spectrum MCC/340; Thermo Scientific) at a wavelength of 365 nm, based on a calibration curve (R^2 = 0.99). Each sample was evaluated in triplicate.

Cytotoxicity Testing

For the in vitro analysis of cytotoxicity, the MCF-7 cell line was obtained from frozen vials of laboratory stock obtained from the ATCC (Manassas, VA, USA). The MCF-7 cells were grown in Dulbecco's modified Eagle medium (DMEM; Gibco) prepared with 1% (v/v) antibiotic and antimycotic solution (ref. 15240062; Gibco) and supplemented with 10% fetal bovine serum (FBS; Gibco), in 75-cm^2 plastic bottles at 37°C in a 95% humid atmosphere with 5% CO_2.

To avoid the interference in the experiment of the action of the steroids present in the FBS, and of the weak estrogenic activity of the phenol red present in the DMEM, the cells were washed with PBS and then medium with 10% carbon-stripped FBS (Sigma) and phenol red–free DMEM was added 48 h before incubation with the nanofibers.

For peripheral-blood mononuclear cell (PBMCs) isolation, 10-mL peripheral blood samples were obtained by venipuncture of the brachial vein from a healthy volunteer who had provided informed consent. The blood was collected into tubes with heparin, and PBMCs were obtained using a Ficoll gradient procedure (Rotstein et al., 1988). Briefly, the 10-mL tubes of blood were centrifuged at 2000 rpm for 5 min, and the buffy coat was then removed with a sterile 2-mL pipette. The buffy coat (2 mL) was added gently to a 15-mL tube with 2 mL Ficoll Histopaque-1077 (Sigma), which was centrifuged without brake for 20 min at 2000 rpm. Then, the white layer was recovered with a sterile 2-mL pipette and placed in a new tube with 5 mL PBX 1X prepared from a 10X solution (ref. 70011044; Gibco), which was centrifuged twice at 2500 rpm for 5 min. The cell pellet was then recovered, gently resuspended, and placed in a new 15-mL tube containing 5 mL PB-MAX karyotyping medium (Invitrogen) with 100 µL phytohemagglutinin (PHA) M (ref. 10576-015; Gibco) and antibiotic and antimycotic solution (ref. 15240062; Gibco). The tube was stored at 37°C and 5% CO_2 for 24 h before nanofibers treatment with. Incomplete statement

The cytotoxicity activity of PCL-TMX nanofibers were evaluated by an indirect contact resazurin assay. The mean absorbance values obtained for all groups were distributed normally, and the control group data were adjusted to 100% viability. Cytotoxicity was calculated based on cell viability relative to this group: none, >90%; slight, 60–90%; moderate, 30–59%; and severe, <30% (Basak et al., 2016). This test indicates the number of viable cells and the level of metabolic activity in a sample. Resazurin, a blue dye, is metabolized by mitochondrial enzymes in cells, which transforms it into fluorescent pink resorufin, which the cells release into the culture medium. Treatments can be monitored by taking several measurements of the same group of cells, as resazurin is not toxic. Plates are removed from the incubator for a short time (5–10 min) to take measurements, and the culture conditions are then restored (Escobar, 2010; Uzarski et al., 2017). The MCF-7 cells were seeded in a 96-well culture plate at a density of 15,000/200 µL for 24 h. Then, a 7mm diameter circle containing approximately 16 µM of TMX was added to each well with 200 µL the culture medium for 1–6 days, in duplicate. Every day, a plate was taken from the incubator and the culture medium was removed; the wells were washed with 200 µL PBS, and fresh serum-free medium with 4.4 µM resazurin was added, followed by further incubation under the same initial conditions. After 4, 6, and 24 h, absorbance was measured at the emission wavelength of 595 nm and excitation wavelength of 535 nm using a spectrophotometer (Cytation 3 (Borra et al., 2009; Uzarski et al., 2017). were

free tamoxifen

An experiment with Tamoxifen free was made, MCF-7 cells were cultured with concentrations of free TMX between (0-20µM), an effect similar on viability percentage to PCL-TMX, was observed with concentrations between 13 and 20 µM (see Supplementary figure). with

For PBMCs assays, 15,000 cells/200 µL were placed in 96-well plates after 24 h culture and incubated with the PCL-P and PCL-TMX nanofibers, for 24 hours. The plates were then centrifuged at 2000 rpm for 5 min, and the medium was replaced with PB-MAX containing 4.4

mM resazurin, followed by further incubation under the same conditions. After 4h, 6h, 24h, 30h and 48h the absorbance was measurement the same way to MCF-7 cells lines.

measured in

as with

Statistical Analysis

The results were organized by treatment: PCL-P, PCL-TMX and without nanofiber and by numbers of resorufin measurements according to cell type. The normality test Shapiro–Wilk was applied, then the treatments were compared using Student's t test for unpaired variables: MCF-7+PCL-P vs. MCF-7+PCL-TMX, MCF-7+PCL-P vs. MCF-7 without nanofiber, MCF-7+PCL-TMX vs. MCF-7 without nanofiber and PBMCs+PCL-P vs. PBMCs+PCL-TMX, PBMCs+PCL-P vs. PBMCs without nanofiber, PBMCs +PCL-TMX vs. PBMCs without nanofiber). Here we found that the PCL-TMX treatment reduced the percentage viability of MCF-7, besides the difference was statistically significant in all measurements ($p \leq 0.05$). One day after PCL-P treatment of MCF-7 cells, the percentage of viability increases slightly and it is statistically significant only in first day at 4h ($p= 0.0160$) and on the sixth day at 24h ($p= 0.0317$), in the latter case, a clone of MCF-7 with a higher proliferation rate probably emerged. PCL-P induced an increase in the percentage of viability of PBMCs on the first day of treatment, even above the cells without treatment, while PCL-TMX reduced it however, applying the Student's *t* test the differences were not significant in the PCL-P treatments, but they were significant for the PCL-TMX at 4h $p = 0.005$ and 6h $p = 0.0243$.

and

Also, ANOVA was applied to three treatments for each cell type (MCF-7+PCL-P vs. MCF7+PCL-TMX vs. MCF-7 without nanofiber and PBMCs +PCL-P vs. PBMCs+PCL-TMX vs. PBMCs without nanofiber). All treatments showed statistically significant differences, but this test does not discriminate between groups. Additionally, BONFERRONI test was used to compare each treatment with no nanofiber addition (MCF-7+PCL-P vs MCF-7 without nanofiber, MCF7+PCL-TMX vs MCF-7 without nanofiber and PBMCs+PCL-P vs PBMCs without nanofiber, PBMCs+PCL-TMX vs. PBMCs without nanofiber). This showed that PCL-P increases the percentage of viability in a statistically significant way except for the 6h data. On the other hand, PCL-TMX decreases this value and only in a statistically significant way for the measurement taken at 24 h.

Results and Discussion

Physicochemical Characterization

SEM showed that all PCL-P and PCL-TMX nanofibers were uniaxial, non-porous, and distributed randomly. The incorporation of TMX altered the nanofiber morphology and diameter (see Fig. 1). The PCL-P nanofibers displayed a bimodal diameter distribution, whereas that of the PCL-TMX nanofibers was modal. The greatest average diameters were 484 ± 168 nm for PCL-P nanofibers

Fig 1 shows only 1 peak.

largest

and 400 ± 236 nm for PCL-TMX nanofibers. The PCL-P nanofiber diameters were comparable to those reported previously (Katsogiannis, Vladisavljević & Georgiadou, 2015), and the reduction of the average diameter with TMX incorporation is consistent with previous reports that drug or particle incorporation reduces PCL nanofiber diameters (Zamani et al., 2010; Aristilde et al., 2010; Monteiro et al., 2017; Alavarse et al., 2017; Pinzón-García et al., 2017).

Figure 1. The morphology and diameter distribution of PCL nanofibers showed in micrographs, and histograms corresponding of PCL nanofibers SEM micrographs of a) PCL, b) PCL-TMX. Histograms of the diameter of nanofibers of c) PCL, d) PCL-TMX. PCL-P

The FTIR-ATR spectra of TMX and the PCL-P and PCL-TMX nanofibers are shown in Fig. 2. TMX showed a band of intensity at 3229 cm^{-1} due to the O–H from alcohol and phenolic groups. The most characteristic TMX bands were observed: the C = O band at 1627 cm^{-1}, the N–H band at 1575 cm^{-1}, the C = C stretching band (reflecting aromatic ring vibrations) at 1453 cm^{-1}, the double amino C–N stretching bands at 1227 cm^{-1}, and the phenolic C–O stretching band at 1174 cm^{-1} (Aristilde et al., 2010; dos Santos Ferreira da Silva et al., 2015). For the PCL-P nanofiber, characteristic infrared bands were observed at 1720 cm^{-1} (C = O carbonyl stretching), 1240 cm^{-1} (asymmetrical C–O–C stretching), 1157 cm^{-1} (symmetrical C–O–C stretching), 2945 cm^{-1} (asymmetrical CH_2 stretching), and 2868 cm^{-1} (symmetrical CH_2 stretching) (Elzein et al., 2004; Gomes et al., 2008). For the PCL-TMX nanofibers, the TMX absorption peaks were not observed, likely due to the small quantity of TMX in them and stretching overlap with adsorption bands of the PCL polymer (Liebenberg et al., 1999; Khalf & Madihally, 2017).

Figure 2. FTIR spectra of TMX, PCL, and PCL-TMX nanofibers. PCL-P

Fig. 3 shows the XRD patterns of TMX and the PCL-P and PCL-TMX nanofibers. TMX showed low-intensity peaks due to its polycrystalline structure; the main peaks were at 2θ = 8.5°, 9.3°, 10.6°, 17.0°, 21.1°, and 23.0° (Liebenberg et al., 1999; Thangadurai et al., 2005; Toro R et al., 2007). All PCL-P nanofibers showed two characteristic peaks at 2θ = 21.25° and 23.55°, attributed to (110) and (200) PCL semicrystalline lattice planes (Baji et al., 2007; Wang, Guo & Cheng, 2008; Kim et al., 2012). No characteristic TMX peak was detected in the PCL-TMX nanofiber pattern. These results can be explained by the lack of time for the polymers and other compounds to crystallize and form organized structures during electrospinning, which is a very rapid method of polymer fiber preparation (Wei et al., 2010).

Figure 3. XRD patterns of (a) TMX, (b) PCL, (c) PCL-TMX

Fig. 4 shows the TG and DTG curves of TMX nanofibers. These curves for TMX showed that three events of mass loss occurred at temperatures of up to 600°C. The first event corresponds to 7.4% mass loss at about 100°C, which can be attributed to dehydration. The second event occurred between 126°C and 380°C, with 34% mass loss (also observed on the DTG curve), and the third event occurred between 400°C and 600°C, with 74% mass loss. These events can be attributed to the oxidative decomposition of TMX and the remaining carbonaceous matter (dos Santos Ferreira da Silva et al., 2015; Cervini et al., 2015). The nanofiber patterns (Fig. 4a, b) were similar to the reported PCL weight loss pattern, which comprises one thermal decomposition event starting at about 340°C and ending at 470°C (Mohamed et al., 2008). The PCL-TMX nanofibers showed greater thermal stability than did the PCL-P nanofibers. The TG curves for the PCL-P and PCL-TMX nanofibers showed that one thermal decomposition event occurred at about 408°C, with complete decomposition occurring by 600°C (Fig. 4c).

In this T range, there are 2 peaks in DTG and 2 wt loss steps in TG. Please check the weight loss values for all steps.

total weight loss only for PCL-P not PCL-TMX at 600C

4a

Figure 4. a) TG, b) DTG and c) temperature difference curves of TMX, PCL-P, and PCL-TMX

The contact angles of the nanofibers surfaces were measured to assess the wettability and hydrophilicity of the nanofibers. Table 1 shows the contact angles for the PCL nanofibers and PCL-TMX nanofibers. The contact angle of the PCL-TMX nanofiber was smaller than that of the PCL-P nanofiber (hydrophobic nature (Madhaiyan et al., 2013; Tiyek et al., 2019)), perhaps due to the highly hydrophilic COO– moiety of citrate TMX on the surface of the former (Huang et al., 2010). Greater nanofiber wettability may improve cell proliferation and biocompatibility (Sharma et al., 2014). In a similar work, the incorporation of 5-FLU, paclitaxel, and other drugs into PCL nanofibers also increased nanofiber hydrophilicity and provided a good release profile (Karuppuswamy et al., 2015; Iqbal et al., 2017).

In Vitro Drug Release

Profiles of cumulative TMX release from the PCL-TMX nanofibers over 14 h are shown in Fig. 5. After 12 h, no TMX signal was detected by UV-vis quantification, reflecting complete TMX release. Thus, to evaluate the kinetics of TMX release from the nanofibers, the cumulative release of the drug was considered in up to 10 h and 12 h, to PCL-TMX. The large surface areas and three-dimensional open porous structures of nanofibers may reduce the constraint on drug diffusion and release (Seeram Ramakrishna, Zamani & Molamma P Prabhakaran, 2013). In addition, the greater hydrophilicity of PCL-TMX nanofibers certainly increased TMX release.

not understandable

Three distinct, sequential stages of TMX release, reflecting different processes of diffusion from the PCL matrix, were observed (Fig. 5a), in accordance with the literature (Varshosaz et al., 2011;

Sohrabi et al., 2013). In the first stage, there was a linear relationship with a very pronounced and moderate slope. A burst effect was seen, with release of approximately 87% of the TMX release in the first hour of the experiment. This initial rapid release may have been due to the accumulation of the TMX molecules at or near the PCL nanofiber surfaces during electrospinning, facilitating TMX release into the media (Zamani et al., 2010). The second stage of release occurred between 1 and 4 h; the release rate decreased gradually, resulting in a moderate slope, as a consequence of TMX diffusion through the PCL nanofibers instead of PCL degradation. The third stage occurred between 4 and 10 h and involved the least TMX release. Thus, sustained TMX release from the PCL-TMX nanofibers was observed up to 14 h. These findings are expected for this type of system because an initial burst of drug release is required to promote a local antitumor effect; the initial dose kills the majority of cancerous cells, and the subsequent controlled release prevents tumor cell growth and proliferation (Ma et al., 2011).

Not as shown in Fig 5a

Figure 5. a) Release profiles of TMX from PCL-TMX nanofibers in PBS pH 7.4 and b) Higuchi equation to TMX release from PCL-TMX nanofiber (Where Mt/M∞ is the fraction of TMX delivery in time t, and K is release speed constant).

The mechanism of TMX release was evaluated using the Higuchi kinetic model, based on Fickian diffusion mechanism (Nie et al., 2009). The Higuchi model of the TMX release mechanism best fit to the data for the first 8 h (Fig. 5b). As this model assumes Fickian diffusion, the cumulative percentage of the drug released (Q) was plotted against the square root of time (t ½), i.e., $Q = K \times t$ ½, where K is the Higuchi rate constant. The results indicated that diffusion along the PCL matrix occurred, and that TMX release was not dominated by polymer erosion, as claimed in previous studies of biodegradable polymers and water-soluble molecules (Luong-Van et al., 2006; Fredenberg et al., 2011).

Other studies of drug-delivery systems for anticancer molecules, such as TMX, have shown sustained release over 10 h (Guimarães et al., 2015), 6 days (Criado-Gonzalez et al., 2019), 8 days (Liu et al., 2016), 14 days, 25 days (Iqbal et al., 2017), and 35 days, with different release mechanisms and cytotoxicity. Formulations of nanofibers loaded with tetracycline hydrochloride (TCH), an antibiotic in the same group as TMX, have shown good cytocompatibility in normal cells (Qi et al., 2013; Ranjbar-Mohammadi et al., 2016; Alavarse et al., 2017). Similarly, in this study, the PCL-TMX nanofibers displayed good biocompatibility and potential for use in the treatment of solid tumors.

Cytotoxicity

The PCL-TMX showed greater cytotoxicity against MCF-7 cells than did the PCL–P (see Fig. 6); 20 % cell viability was observed on the first day, in contrast to the 100% and 127% viability observed in untreated cells and those incubated with PCL-P, respectively. After the second day, resazurin metabolism was barely detected in cells incubated with PCL-TMX; those incubated with PCL-P showed a slight decrease in viability but like no treated cell.

This part is repeated below.

TMX inhibits MCF-7 proliferation (Niro, Hennebert & Morfin, 2010), arresting cells in the G0–G1 phases of the cell cycle. It also activates apoptosis via procaspase 8, followed by events such as an increase in reactive oxygen species and the release of pro-apoptotic factors from the mitochondria. Real-time polymerase chain reaction revealed an increase in FasL mRNA and tumor necrosis factor-α, as well as a decrease in mitochondrial transmembrane potential, after TMX treatment. All these changes are related to the activation of apoptosis (Subramani et al., 2014).

Figure 6. Percentage of MCF-7 cell viability: cytotoxic effect of PCL-P and PCL-TMX on 15.000 MCF-7 cells was evaluated after 1 to 6 days of exposure. The reduction of resazurin to resorufin was followed at 4, 6 and 24 hours. Using Student's t test PCL-TMX reduced the percentage of viability statistically significant in all treatments, identified by * ($p \leq 0.05$). PCL-P treatment was statistically significant by slightly increasing the percentage of viability on the first day at 4h ($p = 0.0160$) and the sixth day at 24h ($p= 0.03117$) and decreasing the third day at 24h ($p= 0.0425$) identified by **.

Afterward 24 h PCL-TMX showed greater cytotoxicity against MCF-7 than did the PCL–P (Fig. 6); 20% ($p= 0.041$) cell viability was observed on the first day, in contrast to the 100% ($p= 0.049$) and 127% ($p= 0.016$) viability observed in untreated cells and those incubated with PCL-P, respectively. This can be explained because the TMX inhibits MCF-7 proliferation (Niro, Hennebert & Morfin, 2010), arresting cells in the G0–G1 phases of the cell cycle. It also activates apoptosis via procaspase 8, followed by events such as an increase in reactive oxygen species and the release of pro-apoptotic factors from the mitochondria. Real-time polymerase chain reaction revealed an increase in FasL mRNA and tumor necrosis factor-α, as well as a decrease in mitochondrial transmembrane potential, after TMX treatment. All these changes are related to the activation of apoptosis (Subramani et al., 2014). After 48h of PCL-TMX incubation, a 99% ($p= 0.016$) reduction in cell viability, representing a significant difference from the other groups, (Supplementary Table S1). On day 6, slight recovery with 2% viability was observed, possibly reflecting the growth of a treatment-resistant clone. MCF-7 cells were cultured with concentrations of free TMX ~~among~~ (0-20μM~~)~~, an effect similar on viability percentage to PCL-TMX, was observed with concentrations between 13 and 20 μM.

when

in the range of

a similar effect

The effect of TMX on PBMCs is not clear. Here we observed a large reduction of viability. The first day the viability percentage reached zero at 4h ($p= 0.050$) and 6h ($p= 0.0243$). On the contrary,

PCL-P increased in viability to 256%, which shows that this polymer could be activated PBMCs proliferation (Fig. 7). In one study, lymphocytes obtained from patients with breast cancer showed no change in cytotoxic activity type natural killer (NK) cells or proliferative response to mitogens after 8 days of TMX treatment (Sheard et al., 1986). This means that TMX does not activate the NK cells from PBMCs ~~neither~~ nor induce their proliferation. In a similar study involving 6–12 months of treatment, a reduced number of lymphocytes with suppressive function was observed (Joensuu, Toivanen & Nordman, 1986). In patients treated with TMX for 1.5–2 years, a decrease in NK cell activity and increase in response to the concanavalin A mitogen were observed (Mandeville, Ghali & Chausseau, 1984). This suggests that if TMX is applied locally, unwanted effects on other tissues can be avoided.

Figure 7. Percentage of PBMCs viability: cytotoxic effect of a) PCL-P and b) PCL-TMX ~~up~~on cultured 15.000 PBMCs for 24 hours. The reduction of resazurin to resorufin was follow-up at 4, 6, 24, 30 and 48 hours. Increase in the percentage of viability was observed with exposure to PCL-P and reduction with PCL-TMX, the statistical significances are identified by *, the values are in the supplementary table S1.

followed up

For PBMCs obtained from the peripheral blood of patients with breast cancer and treated with TMX or left untreated, the response to concanavalin A can take up to 5 days (Rotstein et al., 1988). In this study, PBMCs obtained from the peripheral blood of a healthy volunteer and cultured in the presence of PHA showed detectable metabolic activity in the resazurin assay until the fourth day of culture (Fig. 7). However, lymphocytes in culture under the stimulation of a mitogen such as PHA are viable for about 72 h. The viability of PBMCs increased almost threefold in the presence of PCL-P and decreased by approximately 99% with of PCL-TMX. Little is known about the possible activation and proliferation of PBMCs induced by PCL-P, however they have been used to promote tissue healing in order to promote cell migration (Schoenenberger et al., 2020). In further research, it would be interesting to delve into this aspect. Viability reduction by PCL-TMX is consistent with that reported by Oliveira et al (Oliveira, Genari & Dolder, 2010), who showed cell death due to apoptosis and autophagy in lymphocytes treated with tamoxifen for 24 and 48h, in a time – dependent manner, although they applied a dose of 20 μM while in this study it was 16 μM. They conclude that the effect of TMX on lymphocytes is independent of the estrogen receptor (Behjati & Frank, 2009). Other side effects of TMX are the induction of proliferation in the endometrium, association with liver cancer, increased blood coagulation, retinopathy and corneal opacities formation (Memisoglu-Bilensoy et al., 2005). Among the potential biomedical (drug-delivery) applications of electrospun nanofibers, local postoperative chemotherapy for the prevention of tumor recurrence and metastasis is prominent (Hu et al., 2014). PCL-P is used to administer several types of drugs in the treatment of cancer such as cisplatin, doxycline, curcumin, paclitaxel among others (Malikmammadov et al., 2018), but there are no reports of tamoxifen delivery systems with PCL nanofibers under the conditions described here.

In this study, the PCL-TMX nanofibers displayed good biocompatibility, and thus potential application for the treatment of solid tumors. Similarly, nanofibers loaded with TCH have shown good cytocompatibility in normal cells (Qi et al., 2013; Ranjbar-Mohammadi et al., 2016; Alavarse et al., 2017). Other TMX release systems using nanoparticles achieve 68% release in a first hour (Chawla & Amiji, 2002) then maintains the release until 24hours, while nanofibers released up to 87% of their content in the first time and maintain a sustained release for hours or days, which can give best results. In addition, the destruction of the nanoparticles requires the use of enzymes such as lipases, which can affect the environment of the treated tissue.

Does this refer to Fig 5a? "First time" means "first hour"? See Line 360-361.

Conclusions

PCL-TMX nanofibers were produced effectively by electrospinning and showed sustained TMX release for up to 14 h. In cell viability assays, they exhibited excellent activity against the MCF-7 cell line. These results suggest that PCL-TMX nanofibers have potential application as a drug-delivery local system for adjuvant treatment of solid tumors including breast cancer, that could avoid the collateral effects of TMX treatment in other tissues such as endometrium, liver, cornea or cells such as PBMCs. No previous reports of PLC-TMX nanofiber releasing systems in the literature.

There are

Acknowledgements

The authors would like to acknowledge the financial support from the following Brazilian Research agencies: CAPES, FAPEMIG, CNPq and Center of Microscopy at UFMG, and the Universidad del Rosario and COLCIENCIAS Contract: FP44842-07-2018 Code: 122277657905, supported this work.

References

Alavarse AC, de Oliveira Silva FW, Colque JT, da Silva VM, Prieto T, Venancio EC, Bonvent J-J. 2017. Tetracycline hydrochloride-loaded electrospun nanofibers mats based on PVA and chitosan for wound dressing. *Materials Science and Engineering: C* 77:271–281. DOI: 10.1016/j.msec.2017.03.199.

Aristilde L, Marichal C, Miéhé-Brendlé J, Lanson B, Charlet L. 2010. Interactions of Oxytetracycline with a Smectite Clay: A Spectroscopic Study with Molecular Simulations. *Environmental Science & Technology* 44:7839–7845. DOI: 10.1021/es102136y.

Baji A, Wong S-C, Liu T, Li T, Srivatsan TS. 2007. Morphological and X-ray diffraction studies of crystalline hydroxyapatite-reinforced polycaprolactone. *Journal of Biomedical Materials Research Part B: Applied Biomaterials* 81B:343–350. DOI: 10.1002/jbm.b.30671.

519 Barnes CP, Sell SA, Boland ED, Simpson DG, Bowlin GL. 2007. Nanofiber technology: designing the
520 next generation of tissue engineering scaffolds. *Advanced Drug Delivery Reviews* 59:1413–1433. DOI:
521 10.1016/j.addr.2007.04.022.
522
523 Basak V, Bahar TE, Emine K, Yelda K, Mine K, Figen S, Rustem N. 2016. Evaluation of cytotoxicity
524 and gelatinases activity in 3T3 fibroblast cell by root repair materials. *Biotechnology & Biotechnological*
525 *Equipment* 30:984–990. DOI: 10.1080/13102818.2016.1192960.
526
527 Behjati S, Frank M. 2009. The Effects of Tamoxifen on Immunity. *Current Medicinal Chemistry*
528 16:3076–3080. DOI: 10.2174/092986709788803042.
529
530 Caracciolo, Pablo R Cortez Tornello, Fabián Buffa, Florencia Montini Ballarin, Teresita R Cuadrado,
531 Gustavo A Abraham. 2011. Pequeñas fibras grandes aplicaciones. *Instituto de Investigaciones en Ciencia*
532 *y Tecnología de Materiales, INTEMA (UNMDP-Conicet), Mar del Plata, Argentina* 20:57–64.
533
534 Cervini P, Ambrozini B, Machado LCM, Ferreira APG, Cavalheiro ÉTG. 2015. Thermal behavior and
535 decomposition of oxytetracycline hydrochloride. *Journal of Thermal Analysis and Calorimetry* 121:347–
536 352. DOI: 10.1007/s10973-015-4447-x.
537
538 Chawla JS, Amiji MM. 2002. Biodegradable poly(epsilon -caprolactone) nanoparticles for tumor-targeted
539 delivery of tamoxifen. *International Journal of Pharmaceutics* 249:127–138. DOI: 10.1016/s0378-
540 5173(02)00483-0.
541
542 Criado-Gonzalez M, Fernandez-Gutierrez M, San Roman J, Mijangos C, Hernández R. 2019. Local and
543 controlled release of tamoxifen from multi (layer-by-layer) alginate/chitosan complex systems.
544 *Carbohydrate Polymers* 206:428–434. DOI: 10.1016/j.carbpol.2018.11.007.
545
546 De Clercq E. 2015. Ebola virus (EBOV) infection: Therapeutic strategies. *Biochemical Pharmacology*
547 93:1–10. DOI: 10.1016/j.bcp.2014.11.008.
548
549 Dias AM, da Silva FG, Monteiro AP de F, Pinzón-García AD, Sinisterra RD, Cortés ME. 2019.
550 Polycaprolactone nanofibers loaded oxytetracycline hydrochloride and zinc oxide for treatment of
551 periodontal disease. *Materials Science and Engineering: C* 103:109798. DOI:
552 10.1016/j.msec.2019.109798.
553
554 Donneyong MM, Bykov K, Bosco-Levy P, Dong Y-H, Levin R, Gagne JJ. 2016. Risk of mortality with
555 concomitant use of tamoxifen and selective serotonin reuptake inhibitors: multi-database cohort study.
556 *BMJ* 354:i5014. DOI: 10.1136/bmj.i5014.
557
558 Drăgănescu M, Carmocan C. 2017. Hormone Therapy in Breast Cancer. *Chirurgia (Bucharest, Romania:*
559 *1990)* 112:413–417. DOI: 10.21614/chirurgia.112.4.413.
560 Duque L, Rodriguez, Lopez. 2013. ELECTROSPINNING: LA ERA DE LAS NANOFIBRAS. *Revista*
561 *Iberoamericana de Polímeros* 14:10–27.
562

Elzein T, Nasser-Eddine M, Delaite C, Bistac S, Dumas P. 2004. FTIR study of polycaprolactone chain organization at interfaces. *Journal of Colloid and Interface Science* 273:381–387. DOI: 10.1016/j.jcis.2004.02.001.

Escobar L. 2010. Aplicación de un método fluorométrico para evaluar la proliferación celular en líneas celulares tumorales. *Vitae* 17:173–180.

Fredenberg S, Wahlgren M, Reslow M, Axelsson A. 2011. The mechanisms of drug release in poly(lactic-co-glycolic acid)-based drug delivery systems—A review. *International Journal of Pharmaceutics* 415:34–52. DOI: 10.1016/j.ijpharm.2011.05.049.

Gomes ME, Azevedo HS, Moreira AR, Ellä V, Kellomäki M, Reis RL. 2008. Starch–poly(ε-caprolactone) and starch–poly(lactic acid) fibre-mesh scaffolds for bone tissue engineering applications: structure, mechanical properties and degradation behaviour. *Journal of Tissue Engineering and Regenerative Medicine* 2:243–252. DOI: 10.1002/term.89.

Group (EBCTCG) EBCTC. 2011. Relevance of breast cancer hormone receptors and other factors to the efficacy of adjuvant tamoxifen: patient-level meta-analysis of randomised trials. *The Lancet* 378:771–784. DOI: 10.1016/S0140-6736(11)60993-8.

Guimarães PPG, Oliveira MF, Gomes ADM, Gontijo SML, Cortés ME, Campos PP, Viana CTR, Andrade SP, Sinisterra RD. 2015. PLGA nanofibers improves the antitumoral effect of daunorubicin. *Colloids and Surfaces B: Biointerfaces* 136:248–255. DOI: 10.1016/j.colsurfb.2015.09.005.

Hong JH, Ha KS, Jung YH, Won HS, An HJ, Lee GJ, Kang D, Park JC, Park S, Byun JH, Suh YJ, Kim JS, Park WC, Jung SS, Park IY, Chung S-M, Woo IS. 2016. Clinical Features of Male Breast Cancer: Experiences from Seven Institutions Over 20 Years. *Cancer Research and Treatment* 48:1389–1398. DOI: 10.4143/crt.2015.410.

Hu X, Liu S, Zhou G, Huang Y, Xie Z, Jing X. 2014. Electrospinning of polymeric nanofibers for drug delivery applications. *Journal of Controlled Release* 185:12–21. DOI: 10.1016/j.jconrel.2014.04.018.

Huang FL, Wang QQ, Wei QF, Gao WD, Shou HY, Jiang SD. 2010. Dynamic wettability and contact angles of poly(vinylidene fluoride) nanofiber membranes grafted with acrylic acid. *Express Polymer Letters* 4:551–558. DOI: 10.3144/expresspolymlett.2010.69.

Cancer Today-Globocan. 2018. *Available at http://gco.iarc.fr/today/home* (accessed April 28, 2021).
Iqbal S, Rashid MohammadH, Arbab AliS, Khan M. 2017. Encapsulation of Anticancer Drugs (5-Fluorouracil and Paclitaxel) into Polycaprolactone (PCL) Nanofibers and *In Vitro* Testing for Sustained and Targeted Therapy. *Journal of Biomedical Nanotechnology* 13:355–366. DOI: 10.1166/jbn.2017.2353.

Jain N, Jain GK, Javed S, Iqbal Z, Talegaonkar S, Ahmad FJ, Khar RK. 2008. Recent approaches for the treatment of periodontitis. *Drug Discovery Today* 13:932–943. DOI: 10.1016/j.drudis.2008.07.010.

Joensuu H, Toivanen A, Nordman E. 1986. Effect of tamoxifen on immune functions. *Cancer Treatment Reports* 70:381–382.

Johnston S, Basik M, Hegg R, Lausoontornsiri W, Grzeda L, Clemons M, Dreosti L, Mann H, Stuart M, Cristofanilli M. 2016. Inhibition of EGFR, HER2, and HER3 signaling with AZD8931 in combination with anastrozole as an anticancer approach: Phase II randomized study in women with endocrine-therapy-naïve advanced breast cancer. *Breast Cancer Research and Treatment* 160:91–99. DOI: 10.1007/s10549-016-3979-5.

Joshi D, Garg T, Goyal AK, Rath G. 2016. Advanced drug delivery approaches against periodontitis. *Drug Delivery* 23:363–377. DOI: 10.3109/10717544.2014.935531.

Karn A, Jha AK, Shrestha S, Acharya B, Poudel S, Bhandari RB. 2010. Tamoxifen for breast cancer. *JNMA; journal of the Nepal Medical Association* 49:62–67.

Karuppuswamy P, Reddy Venugopal J, Navaneethan B, Luwang Laiva A, Ramakrishna S. 2015. Polycaprolactone nanofibers for the controlled release of tetracycline hydrochloride. *Materials Letters* 141:180–186. DOI: 10.1016/j.matlet.2014.11.044.

Katsogiannis KAG, Vladisavljević GT, Georgiadou S. 2015. Porous electrospun polycaprolactone (PCL) fibres by phase separation. *European Polymer Journal* 69:284–295. DOI: 10.1016/j.eurpolymj.2015.01.028.

Kedjouar B, de Medina P, Oulad-Abdelghani M, Payre B, Silvente-Poirot S, Favre G, Faye J, Poirot M. 2004. Molecular characterization of the microsomal tamoxifen binding site. *JOURNAL OF BIOLOGICAL CHEMISTRY* 279:34048-34048–34061. DOI: 10.1074/jbc.M405230200.

Khalf A, Madihally SV. 2017. Modeling the permeability of multiaxial electrospun poly(ε-caprolactone)-gelatin hybrid fibers for controlled doxycycline release. *Materials Science and Engineering: C* 76:161–170. DOI: 10.1016/j.msec.2017.03.093.

Kim Y-J, Park MR, Kim MS, Kwon OH. 2012. Polyphenol-loaded polycaprolactone nanofibers for effective growth inhibition of human cancer cells. *Materials Chemistry and Physics* 133:674–680. DOI: 10.1016/j.matchemphys.2012.01.050.

Laurence J, Cooke H, Sikder S. 1990. Effect of tamoxifen on regulation of viral replication and human immunodeficiency virus (HIV) long terminal repeat-directed transcription in cells chronically infected with HIV-1. *Blood* 75:696–703. DOI: 10.1182/blood.V75.3.696.696.

Li S, Cui Z, Li D, Yue G, Liu J, Ding H, Gao S, Zhao Y, Wang N, Zhao Y. 2019. Hierarchically structured electrospinning nanofibers for catalysis and energy storage. *Composites Communications* 13:1–11. DOI: 10.1016/j.coco.2019.01.008.

Liebenberg W, de Villiers MM, Wurster DE, Swanepoel E, Dekker TG, Lötter AP. 1999. The Effect of Polymorphism on Powder Compaction and Dissolution Properties of Chemically Equivalent Oxytetracycline Hydrochloride Powders. *Drug Development and Industrial Pharmacy* 25:1027–1033. DOI: 10.1081/DDC-100102265.

Liu W, Wang Y, Yao J, Shao Z, Chen X. 2016. Tamoxifen-loaded silk fibroin electrospun fibers. *Materials Letters* 178:31–34. DOI: 10.1016/j.matlet.2016.04.177.

Luong-Van E, Grøndahl L, Chua KN, Leong KW, Nurcombe V, Cool SM. 2006. Controlled release of heparin from poly(ε-caprolactone) electrospun fibers. *Biomaterials* 27:2042–2050. DOI: 10.1016/j.biomaterials.2005.10.028.

Ma G, Liu Y, Peng C, Fang D, He B, Nie J. 2011. Paclitaxel loaded electrospun porous nanofibers as mat potential application for chemotherapy against prostate cancer. *Carbohydrate Polymers* 86:505–512. DOI: 10.1016/j.carbpol.2011.04.082.

Madhaiyan K, Sridhar R, Sundarrajan S, Venugopal JR, Ramakrishna S. 2013. Vitamin B12 loaded polycaprolactone nanofibers: A novel transdermal route for the water soluble energy supplement delivery. *International Journal of Pharmaceutics* 444:70–76. DOI: 10.1016/j.ijpharm.2013.01.040.

Malikmammadov E, Tanir TE, Kiziltay A, Hasirci V, Hasirci N. 2018. PCL and PCL-based materials in biomedical applications. *Journal of Biomaterials Science, Polymer Edition* 29:863–893. DOI: 10.1080/09205063.2017.1394711.

Mandeville R, Ghali SS, Chausseau J-P. 1984. In vitro stimulation of human NK activity by an estrogen antagonist (tamoxifen). *European Journal of Cancer and Clinical Oncology* 20:983–985. DOI: 10.1016/0277-5379(84)90174-3.

Mandlekar S, Kong A-NT. 2001. Mechanisms of tamoxifen-induced apoptosis. *Apoptosis* 6:469-469–477. DOI: 10.1023/A:1012437607881.

Medina P, Favre G, Poirot M. 2004. Multiple Targeting by the Antitumor Drug Tamoxifen: A Structure-Activity Study. *Current Medicinal Chemistry-Anti-Cancer Agents* 4:491–508. DOI: 10.2174/1568011043352696.

Memisoglu-Bilensoy E, Vural I, Bochot A, Renoir JM, Duchene D, Hıncal AA. 2005. Tamoxifen citrate loaded amphiphilic β-cyclodextrin nanoparticles: In vitro characterization and cytotoxicity. *Journal of Controlled Release* 104:489–496. DOI: 10.1016/j.jconrel.2005.03.006.

Mochane MJ, Motsoeneng TS, Sadiku ER, Mokhena TC, Sefadi JS. 2019. Morphology and Properties of Electrospun PCL and Its Composites for Medical Applications: A Mini Review. *Applied Sciences* 9:2205. DOI: 10.3390/app9112205.

Mohamed A, Finkenstadt VL, Gordon SH, Biresaw G, Palmquist DE, Rayas-Duarte P. 2008. Thermal properties of PCL/gluten bioblends characterized by TGA, DSC, SEM, and infrared-PAS. *Journal of Applied Polymer Science* 110:3256–3266. DOI: 10.1002/app.28914.

Monteiro APF, Caminhas LD, Ardisson JD, Paniago R, Cortés ME, Sinisterra RD. 2017. Magnetic nanoparticles coated with cyclodextrins and citrate for irinotecan delivery. *Carbohydrate Polymers* 163:1–9. DOI: 10.1016/j.carbpol.2016.11.091.

Nie H-L, Ma Z-H, Fan Z-X, Branford-White CJ, Ning X, Zhu L-M, Han J. 2009. Polyacrylonitrile fibers efficiently loaded with tamoxifen citrate using wet-spinning from co-dissolving solution. *International Journal of Pharmaceutics* 373:4–9. DOI: 10.1016/j.ijpharm.2009.03.022.

Niro S, Hennebert O, Morfin R. 2010. New insights into the protective effects of DHEA1). *Hormone Molecular Biology & Clinical Investigation* 4:489-489–498. DOI: 10.1515/HMBCI.2010.050.

Oliveira NFP de, Genari SC, Dolder H. 2010. Cell death induced by tamoxifen in human blood lymphocytes cultivated *in vitro* - doi: 10.4025/actascibiolsci.v32i4.7015. *Acta Scientiarum. Biological Sciences* 32:415–421. DOI: 10.4025/actascibiolsci.v32i4.7015.

Pinzón-García AD, Cassini-Vieira P, Ribeiro CC, de Matos Jensen CE, Barcelos LS, Cortes ME, Sinisterra RD. 2017. Efficient cutaneous wound healing using bixin-loaded PCL nanofibers in diabetic mice: Efficient Cutaneous Wound Healing. *Journal of Biomedical Materials Research Part B: Applied Biomaterials* 105:1938–1949. DOI: 10.1002/jbm.b.33724.

Qi R, Guo R, Zheng F, Liu H, Yu J, Shi X. 2013. Controlled release and antibacterial activity of antibiotic-loaded electrospun halloysite/poly(lactic-co-glycolic acid) composite nanofibers. *Colloids and Surfaces B: Biointerfaces* 110:148–155. DOI: 10.1016/j.colsurfb.2013.04.036.

Ramírez-Agudelo R, Scheuermann K, Gala-García A, Monteiro APF, Pinzón-García AD, Cortés ME, Sinisterra RD. 2018. Hybrid nanofibers based on poly-caprolactone/gelatin/hydroxyapatite nanoparticles-loaded Doxycycline: Effective anti-tumoral and antibacterial activity. *Materials Science and Engineering: C* 83:25–34. DOI: 10.1016/j.msec.2017.08.012.

Ranjbar-Mohammadi M, Zamani M, Prabhakaran MP, Bahrami SH, Ramakrishna S. 2016. Electrospinning of PLGA/gum tragacanth nanofibers containing tetracycline hydrochloride for periodontal regeneration. *Materials Science and Engineering: C* 58:521–531. DOI: 10.1016/j.msec.2015.08.066.

Robinson E, Rubin D, Mekori T, Segal R, Pollack S. 1993. In vivo modulation of natural killer cell activity by tamoxifen in patients with bilateral primary breast cancer. *Cancer immunology, immunotherapy: CII* 37:209–212. DOI: 10.1007/BF01525437.

Rogina A. 2014. Electrospinning process: Versatile preparation method for biodegradable and natural polymers and biocomposite systems applied in tissue engineering and drug delivery. *Applied Surface Science* 296:221–230. DOI: 10.1016/j.apsusc.2014.01.098.

Rotstein S, Blomgren H, Petrini B, Wasserman J, von Stedingk LV. 1988. Influence of adjuvant tamoxifen on blood lymphocytes. *Breast Cancer Research and Treatment* 12:75–79. DOI: 10.1007/BF01805743.

Salami S, Karami-Tehrani F. 2003. Biochemical studies of apoptosis induced by tamoxifen in estrogen receptor positive and negative breast cancer cell lines. *Clinical Biochemistry* 36:247–253. DOI: 10.1016/S0009-9120(03)00007-9.

Salman, Falah Hasan Obayes AL-Khikani, Raghdah Maytham Hameed, Younus Jasim Abdullah, Mohanad Kadhim Mirdan Al-Ibraheemi, Atyaf Ali Al-Asadi. 2020. Tamoxifen from chemotherapy to antiviral drug: Possible activity against COVID-19. *Biomedical and Biotechnology Research Journal* 4:108-108–116. DOI: 10.4103/bbrj.bbrj_53_20.

dos Santos Ferreira da Silva J, López Malo D, Anceski Bataglion G, Nogueira Eberlin M, Machado Ronconi C, Alves Júnior S, de Sá GF. 2015. Adsorption in a Fixed-Bed Column and Stability of the Antibiotic Oxytetracycline Supported on Zn(II)-[2-Methylimidazolate] Frameworks in Aqueous Media. *PLOS ONE* 10:e0128436. DOI: 10.1371/journal.pone.0128436.

Schoenenberger AD, Tempfer H, Lehner C, Egloff J, Mauracher M, Bird A, Widmer J, Maniura-Weber K, Fucentese SF, Traweger A, Silvan U, Snedeker JG. 2020. Macromechanics and polycaprolactone fiber organization drive macrophage polarization and regulate inflammatory activation of tendon in vitro and in vivo. *Biomaterials* 249:120034. DOI: 10.1016/j.biomaterials.2020.120034.

Seeram Ramakrishna, Zamani M, Molamma P Prabhakaran. 2013. Advances in drug delivery via electrospun and electrosprayed nanomaterials. *International Journal of Nanomedicine*:2997. DOI: 10.2147/IJN.S43575.

Sestak I, Kealy R, Edwards R, Forbes J, Cuzick J. 2006. Influence of hormone replacement therapy on tamoxifen-induced vasomotor symptoms. *Journal of Clinical Oncology: Official Journal of the American Society of Clinical Oncology* 24:3991–3996. DOI: 10.1200/JCO.2005.04.3745.

Sharma J, Zhang X, Sarker T, Yan X, Washburn L, Qu H, Guo Z, Kucknoor A, Wei S. 2014. Biocompatible electrospun tactic poly(methyl methacrylate) blend fibers. *Polymer* 55:3261–3269. DOI: 10.1016/j.polymer.2014.05.028.

Sheard CR, Reilly F, Tee DE, Vergani D, Lowe D, Baum M, Cameron AE. 1986. The effect of adjuvant cyclophosphamide or tamoxifen on the numbers of lymphocytes bearing T cell or NK cell markers. *British Journal of Cancer* 54:705–709. DOI: 10.1038/bjc.1986.230.

Sohrabi A, Shaibani PM, Etayash H, Kaur K, Thundat T. 2013. Sustained drug release and antibacterial activity of ampicillin incorporated poly(methyl methacrylate)–nylon6 core/shell nanofibers. *Polymer* 54:2699–2705. DOI: 10.1016/j.polymer.2013.03.046.

Song R, Murphy M, Li C, Ting K, Soo C, Zheng Z. 2018. Current development of biodegradable polymeric materials for biomedical applications. *Drug Design, Development and Therapy* Volume 12:3117–3145. DOI: 10.2147/DDDT.S165440.

Subramani T, Yeap SK, Ho WY, Ho CL, Omar AR, Aziz SA, Rahman NMohdANAbd, Alitheen NB. 2014. Vitamin C suppresses cell death in MCF-7 human breast cancer cells induced by tamoxifen. *Journal of Cellular and Molecular Medicine* 18:305–313. DOI: 10.1111/jcmm.12188.

Thangadurai S, Abraham JT, Srivastava AK, Nataraja Moorthy M, Shukla SK, Anjaneyulu Y. 2005. X-Ray Powder Diffraction Patterns for Certain .BETA.-Lactam, Tetracycline and Macrolide Antibiotic Drugs. *Analytical Sciences* 21:833–838. DOI: 10.2116/analsci.21.833.

Tiyek I, Gunduz A, Yalcinkaya F, Chaloupek J. 2019. Influence of Electrospinning Parameters on the Hydrophilicity of Electrospun Polycaprolactone Nanofibres. *Journal of Nanoscience and Nanotechnology* 19:7251–7260. DOI: 10.1166/jnn.2019.16605.

Toro R, de Delgado GD, Bahsas A, Delgado JM. 2007. The presence of polymorphism in oxytetracycline hydrochloride shown by X-ray powder diffraction techniques. :563–568.

Uzarski JS, DiVito MD, Wertheim JA, Miller WM. 2017. Essential design considerations for the resazurin reduction assay to noninvasively quantify cell expansion within perfused extracellular matrix scaffolds. *Biomaterials* 129:163–175. DOI: 10.1016/j.biomaterials.2017.02.015.

Varshosaz J, Jannesari M, Morshed M, Zamani M. 2011. Composite poly(vinyl alcohol)/poly(vinyl acetate) electrospun nanofibrous mats as a novel wound dressing matrix for controlled release of drugs. *International Journal of Nanomedicine*:993. DOI: 10.2147/IJN.S17595.

Venugopal J, Zhang YZ, Ramakrishna S. 2005. Fabrication of modified and functionalized polycaprolactone nanofibre scaffolds for vascular tissue engineering. *Nanotechnology* 16:2138–2142. DOI: 10.1088/0957-4484/16/10/028.

Vitchuli N, Shi Q, Nowak J, Kay K, Caldwell JM, Breidt F, Bourham M, McCord M, Zhang X. 2011. Multifunctional ZnO/Nylon 6 nanofiber mats by an electrospinning–electrospraying hybrid process for use in protective applications. *Science and Technology of Advanced Materials* 12:055004. DOI: 10.1088/1468-6996/12/5/055004.

Vyas SP, Sihorkar V, Mishra V. 2000. Controlled and targeted drug delivery strategies towards intraperiodontal pocket diseases. *Journal of Clinical Pharmacy and Therapeutics* 25:21–42. DOI: 10.1046/j.1365-2710.2000.00261.x.

Wang S, Guo S, Cheng L. 2008. Disodium norcantharidate loaded poly(ε-caprolactone) microspheres. *International Journal of Pharmaceutics* 350:130–137. DOI: 10.1016/j.ijpharm.2007.08.030.

Wei A, Wang J, Wang X, Wei Q, Ge M, Hou D. 2010. Preparation and characterization of the electrospun nanofibers loaded with clarithromycin. *Journal of Applied Polymer Science* 118:346–352. DOI: 10.1002/app.32363.

Zamani M, Morshed M, Varshosaz J, Jannesari M. 2010. Controlled release of metronidazole benzoate from poly ε-caprolactone electrospun nanofibers for periodontal diseases. *European Journal of Pharmaceutics and Biopharmaceutics* 75:179–185. DOI: 10.1016/j.ejpb.2010.02.002.

Figure 1

morphology and diameter distribution.

The morphology and diameter distribution of PCL nanofibers showed in micrographs, and histograms corresponding of PCL nanofibers SEM micrographs of a) PCL-P, b) PCL-TMX. Histograms of the diameter of nanofibers of c) PCL-P, d) PCL-TMX.

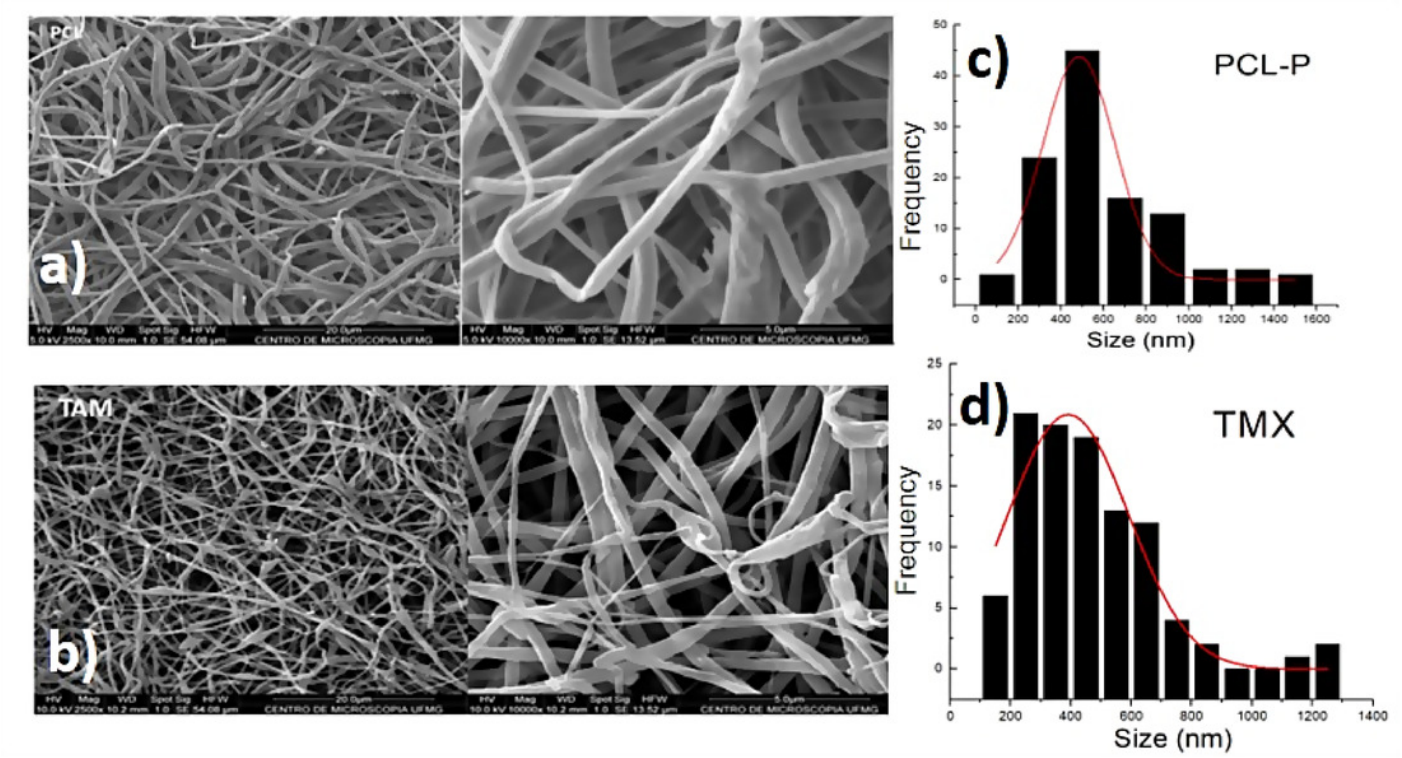

Figure 2

FTIR spectra

FTIR spectra of TMX, PCL-P, and PCL-TMX electrospun nanofibers.

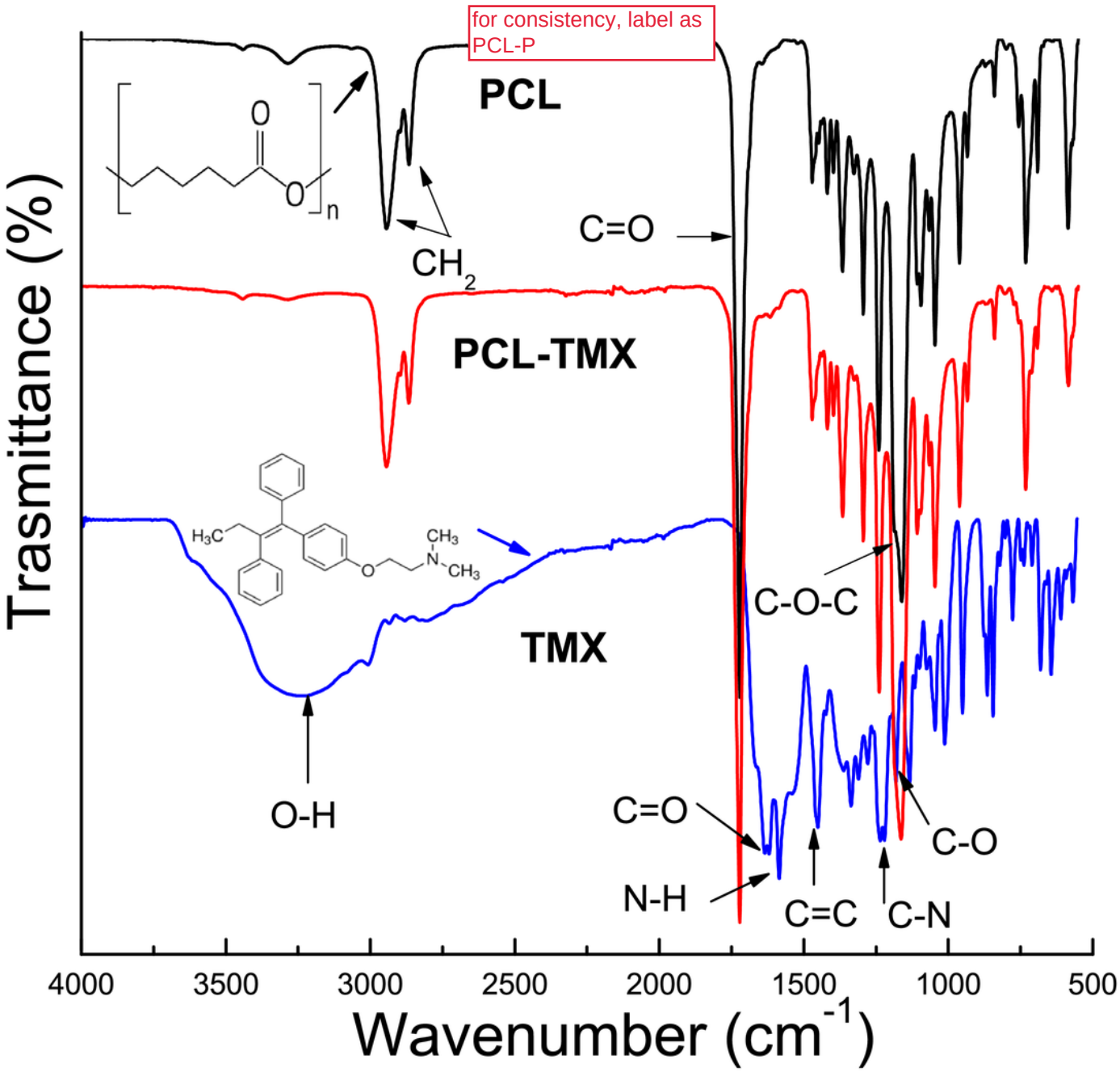

Figure 3

XRD.

XRD patterns of (a) TMX, (b) PCL-P, (c) PCL-TMX

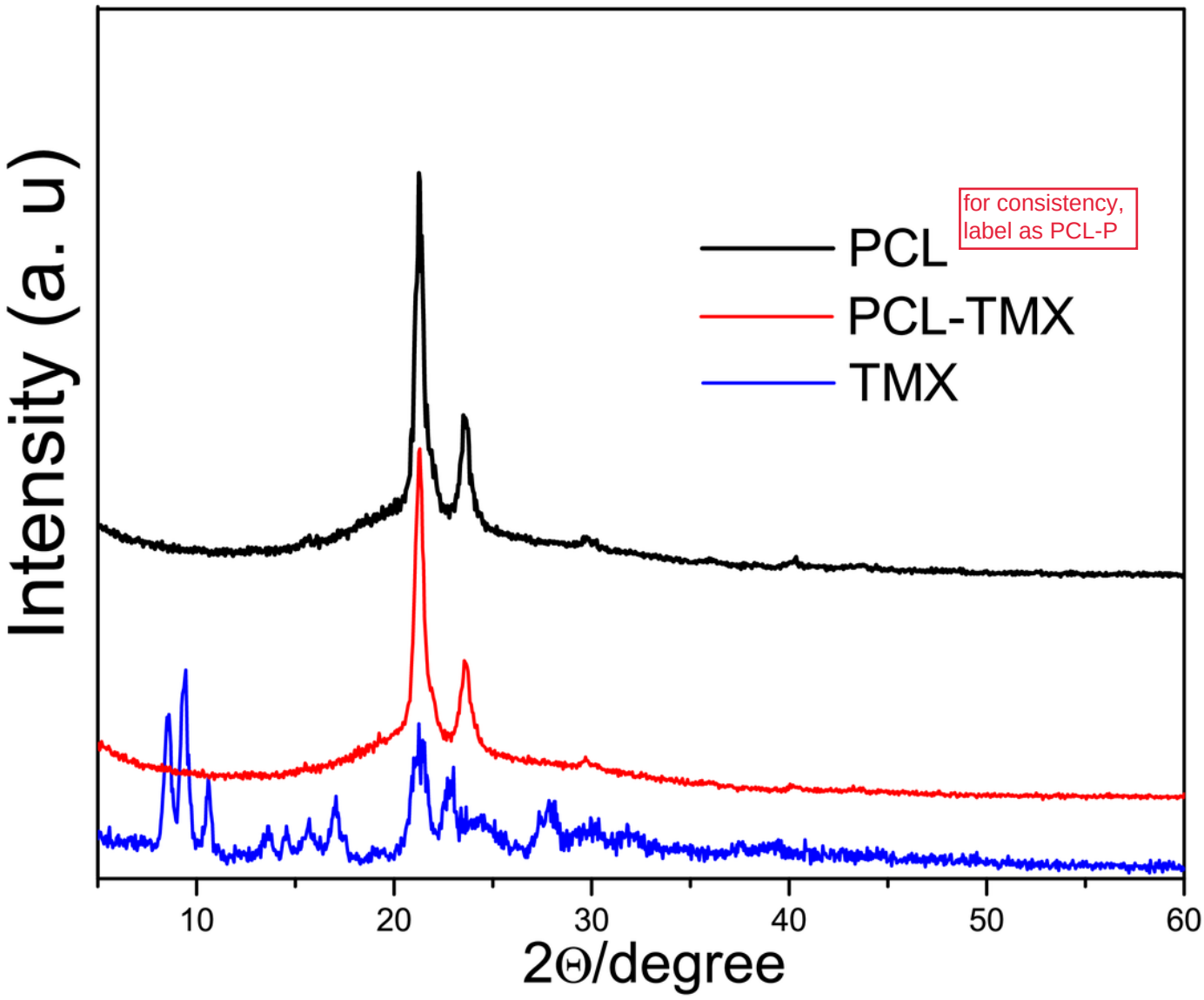

Figure 4

Thermogravimetric analysis.

a) TG, b) DTG and c) temperature difference curves of TMX, PCL-P, and PCL-TMX

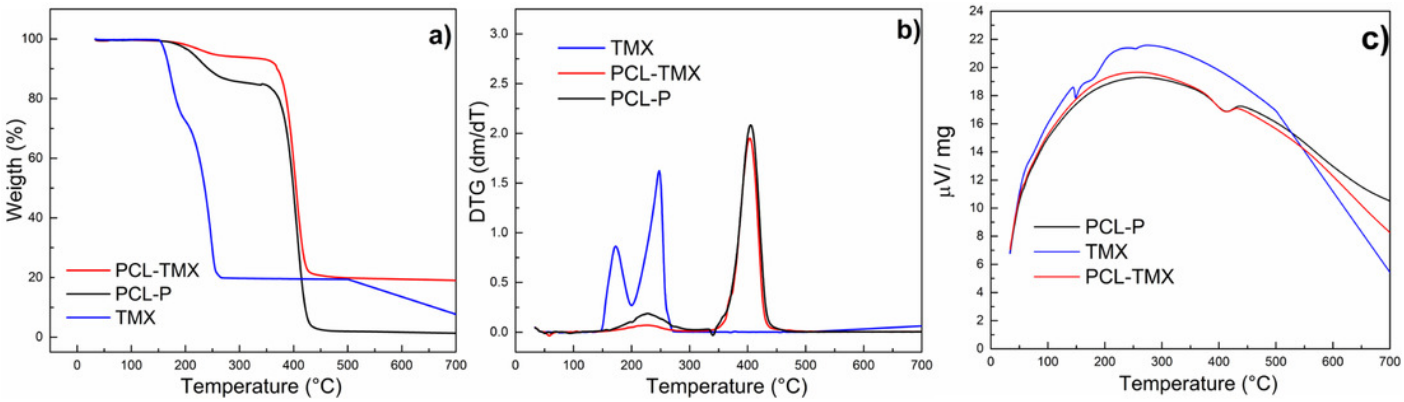

Figure 5

Drug release.

a) Release profiles of TMX from PCL-TMX nanofibers in PBS pH 7.4 and b) Higuchi equation to TMX release from PCL-TMX nanofiber (Where M_t/M_∞ is the fraction of TMX delivery in time t, and K is release speed constant).

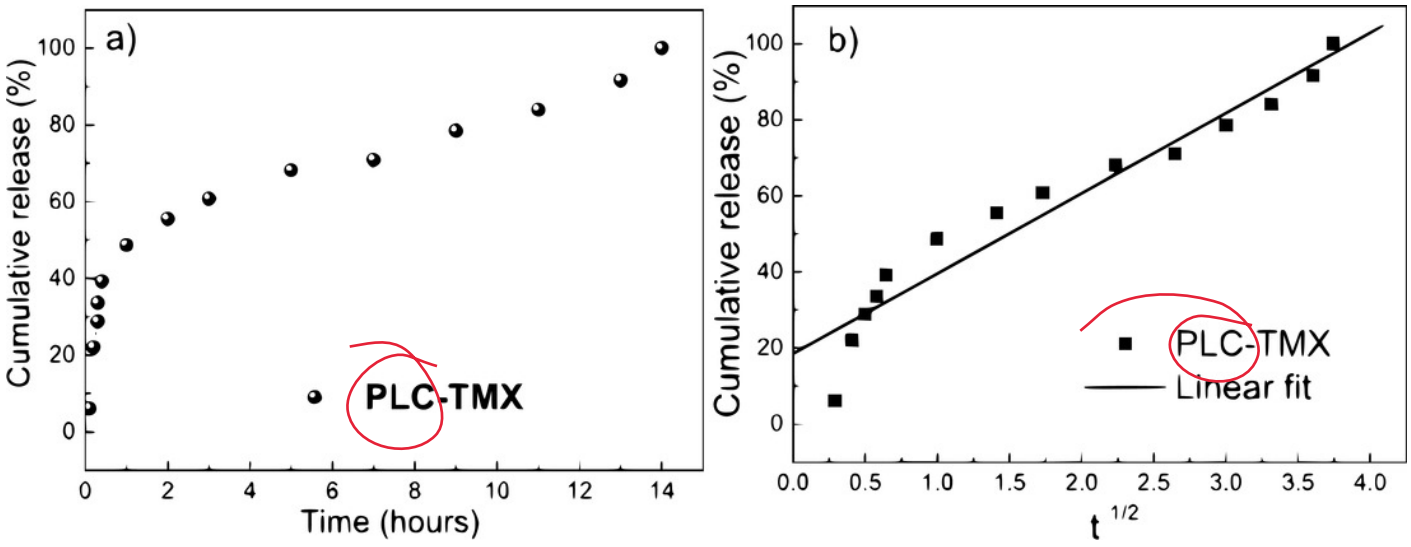

Figure 6

Cytotoxicity assay.

Percentage of MCF-7 cell viability: cytotoxic effect of PCL-P and PCL-TMX on 15.000 MCF-7 cells was evaluated after 1 to 6 days of exposure. The reduction of resazurin to resorufin was followed at 4, 6 and 24 hours. Using Student's t test PCL-TMX reduced the percentage of viability statistically significant in all treatments, identified by * ($p \leq 0.05$). PCL-P treatment was statistically significant by slightly increasing the percentage of viability on the first day at 4h ($p = 0.0160$) and the sixth day at 24h ($p= 0.03117$) and decreasing the third day at 24h ($p= 0.0425$) identified by **.

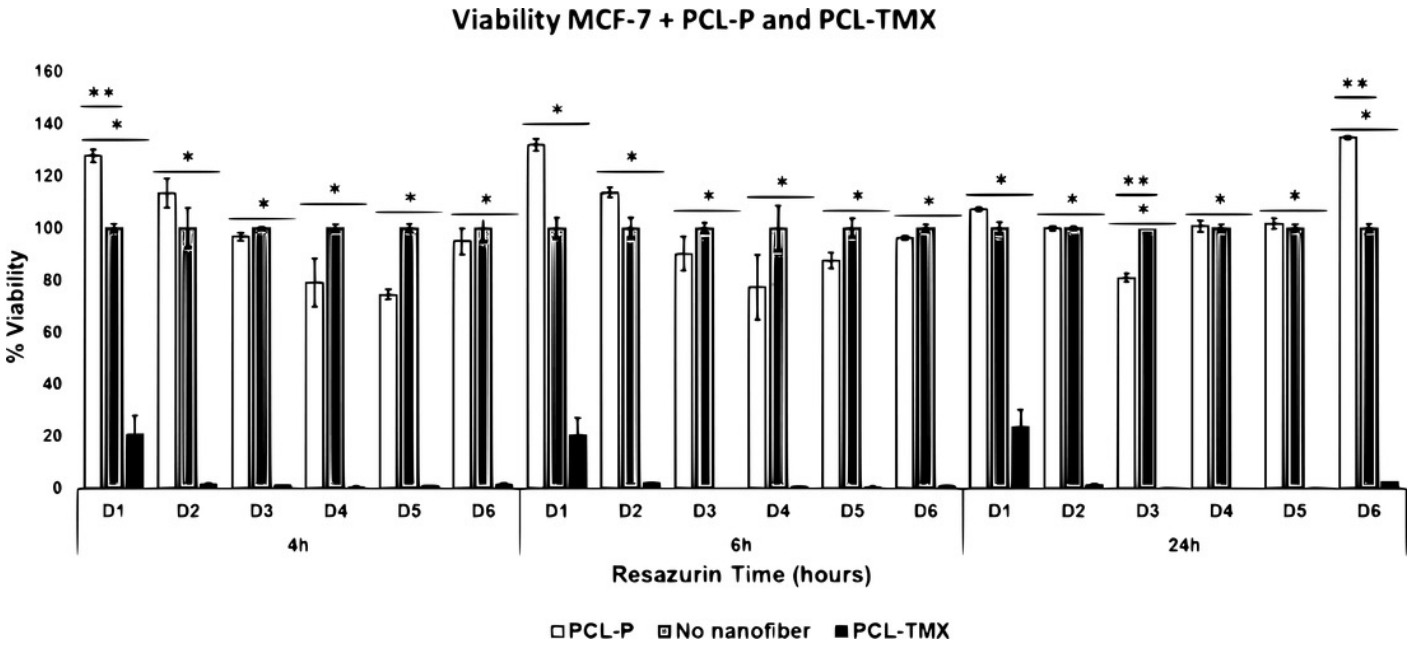

Figure 7

Percentage of PBMCs viability

Percentage of PBMCs viability: cytotoxic effect of a) PCL-P and b) PCL-TMX ~~up~~ followed up on cultured 15.000 PBMCs for 24 hours. The reduction of resazurin to resorufin was follow-up at 4, 6, 24, 30 and 48 hours. Increase in the percentage of viability was observed with exposure to PCL-P and reduction with PCL-TMX, the statistical significances are identified by *, the values are in the supplementary table S1.

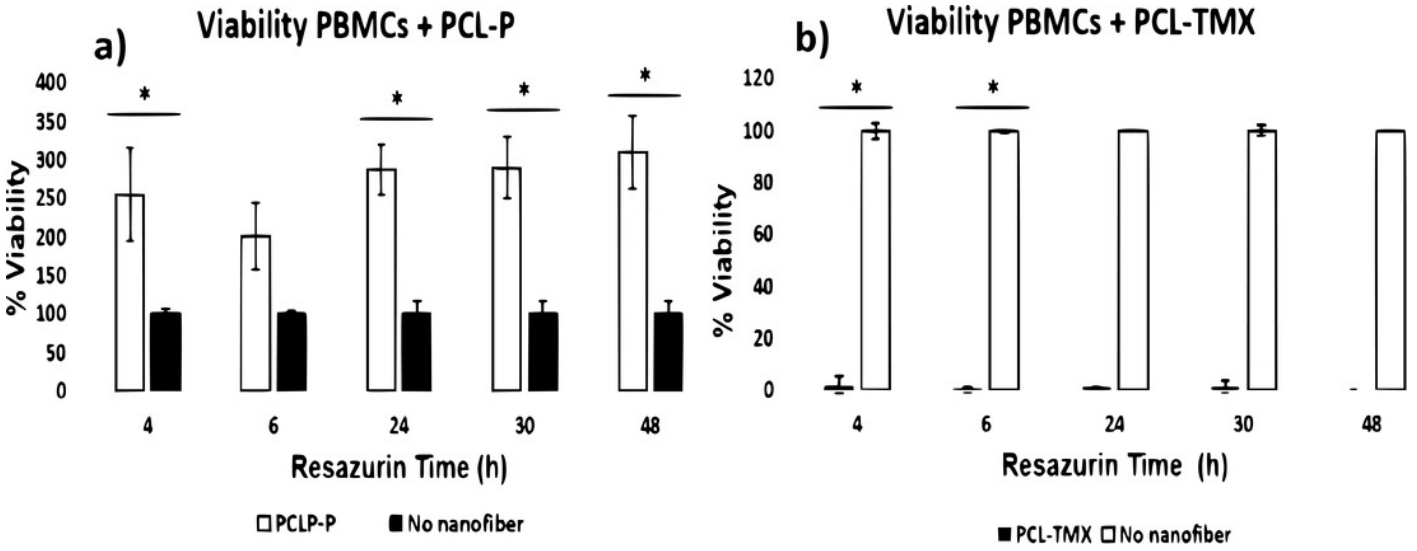

Table 1(on next page)

Contact angle.

Contact angle of the PCL nanofibers after 1s and 120s.

Nanofibers	Time /s	Contact angle / degrees
PCL-P	1	105.75
	120	96.58
PCL-TMX	1	55.79
	120	32.54

1